Weakly nonlinear analysis of symmetry breaking in cell polarity models

Boris Rubinstein[1,†][*], Brian D. Slaughter[1] and Rong Li[1,2]
[1]Stowers Institute for Medical Research,
1000 E 50th St, Kansas City, MO 64110, USA
[2] Department of Molecular and Integrative Physiology
University of Kansas Medical Center,
3901 Rainbow Blvd., Kansas City, KS 66160, USA

February 10, 2012

Abstract

Spontaneous symmetry breaking leading to polarization of the cell is a key step initiating many morphogenetic processes. In addition to experimental studies model-based theoretical description helps to understand the conditions and limitations of this process. Such description is limited usually to linear stability analysis supplied by the numerical simulations to establish the dependence of the polarization dynamics on the model parameters. Here we describe application of a powerful weakly nonlinear analysis method to a minimalistic model characterized by the conservation of mass of the protein governing the polarization dynamics.

PACS numbers: 87.18.Hf, 05.45-a

[*]Corresponding author: bru@stowers.org

1   Introduction

Rho GTPases are conserved regulators of various cellular processes, such as polarization, motility, and asymmetric cell division. In general, they exert their role in these processes by controlling the timing and location of activation of cytoskeleton components. This includes the control over actin polymerization, actomyosin contraction, cell adhesion, and microtubule constancy [1]. Rho GTPases are active when bound to GTP, and inactive when bound to GDP. The exchange of GDP for GTP is catalyzed by their respective guanine nucleotide exchange factors (GEFs), while hydrolysis of GTP to GDP is accomplished through activity of GTPase activating proteins (GAPs). The localization of Rho GTPases is governed by membrane diffusion and various vesicular and cytosolic trafficking mechanisms. Understanding the mechanisms that control the location and activity of Rho GTPases is critical for our understanding of cellular processes that must be spatially restricted to be effective.

The study of this process, starting from the symmetry breaking leading to polarization [2], is far from complete due to large number of interacting components involved. Theoretical analysis of cell polarization is mainly focused on simple models describing dynamics of a selected few proteins [3, 4]. In the extreme case the corresponding models consider only a single protein such as Cdc42 GTPase in both active and inactive form with the assumption that the total amount of this protein is conserved. These minimalistic models [5]-[7] take into account the simple kinetics of two protein forms together with their diffusion and thus they belong to *mass-conserved reaction-diffusion model*. They are characterized by different reaction terms but have one important common feature, namely, the diffusion coefficients for two forms of the protein are at different scales, so their ratio strongly differs from unity.

Standard analysis of such models starts with linear stability analysis of the basic uniform steady state. Linear stability analysis is based on an assumption of smallness of the perturbation amplitude compared to that of the basic state [8, 9]. This step enables one to find conditions for which the stability of the uniform state is compromised and the system evolves to a new steady state corresponding to a polarized cell and also determines the characteristic size (wavelength) of the fastest growing perturbation. If it is much larger in comparison to the characteristic domain size one has a transition to a new spatially uniform state. When the perturbation wavelength is comparable or smaller than the domain size, one has Turing type instability leading to formation of spatially nonuniform structure.

By its nature the linear analysis makes no prediction about the transition process itself, as it describes only the initial phase of small perturbation growth. This is the reason why the transition to the new spatially nonuniform state is usually simulated numerically so that the dependence of the emerging state characteristics on the model parameters can be obtained by performing a large number of simulations. This approach was used in [4] where all the mentioned models had been considered. It should be noted that the models in [5] and [6] were shown to demonstrate Turing type instability that leads to emergence of periodic structure with finite wavelength. On the other hand, the model considered in [7] is known to have a different behavior called *wave-pinning* leading to establishment of sharp spatial boundary between two stable states. In this case the activation wave initiated at the domain edge starts to move towards the other edge, slows down and eventually stops inside the domain. As a result, the detectable difference in protein activity level is created in two compartments of the cell.

The numerical simulation approach is understandably limited in the ability to predict the dynamics of a perturbed state as a function of the model parameter values. This method is indispensable in the case when the perturbation grows infinitely, so that the assumption about its smallness used in linear analysis is no longer valid. In other cases when the perturbation amplitude eventually reaches some finite (saturation) value the amplitude dynamics of this new stationary nonuniform state can

be obtained by means of weakly nonlinear analysis [8, 10]. This approach provides an approximate analytical description of the perturbation dynamics based on the Galerkin method. The spatial profile is presented as a superposition of several spatial modes with different wavelengths where each mode has its own time dependent amplitude. The method's main goal is to obtain a system of differential equations describing the amplitudes dynamics. As a result the original spatio-temporal model represented by partial differential equations reduces to a system of ordinary differential equations (ODEs) that can be solved much faster with higher precision. In some cases this system of ODEs can be reduced even further down to a single *Landau equation* that represents the dynamics of amplitude of the fastest growing mode found at the linear stability analysis step.

The Landau equation implies that the perturbation amplitude change has both linear and nonlinear (usually cubic) contributions. The linear term is always positive, and the amplitude dynamics strongly depends on the sign of the nonlinear term. If this term is positive too, the perturbation grows infinitely so that the assumption of amplitude smallness breaks.

When the nonlinear term is negative its contribution would balance the linear term and the perturbation amplitude reaches some constant *saturation* value that depends on both linear and nonlinear term coefficient. In this case one can find a dependence of this saturation amplitude on all model parameters. It is important to underline that analysis of the Landau equation produces conditions on the parameters for which the saturation can happen.

In this review (which can also be viewed as a tutorial) we present a very detailed analysis for a simple model proposed in [5] which is described in Section 2. The linear stability analysis that includs the description of the fastest growing mode of perturbation is given in Section 3. We show that the model dynamics in linear approximation depends on two dimensionless parameters responsible for diffusive and reactive components of the system. In Section 4 we present weakly nonlinear analysis of the model and derive the conditions for existence of the nonuniform periodic steady state emerging due to symmetry breaking of Turing type. The main result of this Section is a derivation and complete analysis of the Landau equation for the perturbation amplitude. We show existence of four qualitatively different types of evolution of small perturbation depending on the value of the bifurcation parameter. In Section 5 we compare analytical predictions of both linear and weakly nonlinear analyses to results of numerical simulations and show that all predicted regimes are actually observed in numerical experiment.

2 Mass-conserved reaction-diffusion model

In the model of Otsuji et. al. [5], six equations describing the relationship of activation and localization of Rac, Cdc42, and RhoA are used. These equations include Cdc42 activation of Rac, RhoA inhibition of Rac, and co-inhibition of RhoA by both Cdc42 and Rac. This inter-dependency is important for various processes such as migrating epithelial cells or fibroblasts, where Rac and Cdc42 drive cytoskeleton extension at the cell front that drives motility, and RhoA activation in the back of the cell drives membrane retraction and loosening of cellular adhesions [1, 11]. The model also includes the activation of these by their respective GEF's and the inhibition by the respective GAP's. Each GTPase is assumed to be both cytosolic (GDP bound) and membrane (GTP bound) forms. Furthermore, the GTP membrane form undergoes slower diffusion than the GDP bound form. Following perturbation, the reaction-diffusion model was found to form a single polarized distribution following perturbation. After an initial state with multiple polarized sites, a final solution is acquired with distribution of active Rac overlapping with that of Cdc42, while Rho accumulation was limited in the polarized area [5].

The authors simplified the system to describe a single protein with two equations, a mass con-

served reaction-diffusion system. The membrane bound form is assumed to be inactive, and diffuse more slowly than the inactive, cytosolic form. In addition to diffusion, another term, the reaction term $f(u,v)$, was necessary to transform a uniform distribution to a system with a singular polarized distribution following perturbation. The authors showed that the numerical simulations of the simplified model produce solutions similar to that of the original model. In [6] the authors presented as eight-variable model that they also reduced to a mass-conserved reaction-diffusion system of two equations only.

With a simplified mathematical system, it is possible to ask additional questions about the relationship between the size of the perturbation and the resulting polarized state. In previous models, linear analysis resulted in a perturbation that grew in time, always leading to a single solution. However, we provide a tutorial to demonstrate that through non-linear analysis, this system of two equations is able to predict oscillatory behaviors under some conditions. In the context of biology, this result demonstrates how a reaction-diffusion system may lead to a periodic polarized system.

The dynamics of two variables u and v representing the active and inactive form of the protein is described by the one-dimensional reaction-diffusion equations in a region $0 \leq x \leq L$

$$\frac{\partial u}{\partial t} = D_u \frac{\partial^2 u}{\partial x^2} + f(u,v), \tag{1}$$

$$\frac{\partial v}{\partial t} = D_v \frac{\partial^2 v}{\partial x^2} - f(u,v), \tag{2}$$

where it is assumed that the diffusion of the membrane-bound active form is much slower than the inactive one: $D_u \ll D_v$. The function $f(u,v)$ describes the reaction term depending on concentration of both forms. A specific expression of the reaction term depends on the model but the dynamics of at least the active form should be nonlinear to make symmetry breaking possible. As an example we use the reaction model discussed in [5], which has a form

$$f(u,v) = a_1 \left[v - \frac{u+v}{(a_2(u+v)+1)^2} \right], \tag{3}$$

where u and v denote active and inactive form of RhoGTPase protein. The first term in (3) stands for the conversion of the inactive form into the active one with the rate a_1, while the second term is responsible for the reverse reaction described by a nonlinear function of total protein concentration; a_2 is the bifurcation parameter determining the stability of the basic uniform steady state.

Assuming no-flux (or periodic) boundary conditions on both ends of the interval one can sum the equations (1,2) and integrate over the spatial variable to obtain the protein mass conservation condition

$$\int_0^L (u+v)dx = CL = const, \tag{4}$$

where the constant C is the model parameter representing the mean protein concentration.

The basic stationary spatially uniform positive solution $\{u_0, v_0\}$ verifies the equation $f(u_0, v_0) = 0$. From (4) it follows that the basic solution satisfies the condition $u_0 + v_0 = C$. Using this condition we obtain for the basic solution

$$u_0 = \frac{A_2(A_2+2)C}{(A_2+1)^2}, \quad v_0 = \frac{C}{(A_2+1)^2}, \quad A_2 = a_2(u_0+v_0) = a_2 C, \tag{5}$$

It appears that for some parameter values this basic state can be unstable to small spatially periodic perturbations. Linear stability analysis determines the range of parameters values in which

4

the basic state stability is lost; it also produces the wavelength of the most unstable perturbation and predicts its growth rate valid at the initial stage of perturbation evolution when its amplitude is small compared to the basic state value.

3 Linear stability analysis

3.1 Perturbation dynamics

Consider stability of the basic state with respect to small perturbations. Define a perturbed state

$$u = u_0 + u_1(x,t), \quad v = v_0 + v_1(x,t), \tag{6}$$

where the perturbation amplitude of each component is much smaller than the corresponding basic value: $|u_1| \ll u_0$, $|v_1| \ll v_0$. Substituting expressions (6) into equations (1,2), expanding them in the Taylor series around the basic state and retaining the linear term in perturbations we find

$$\frac{\partial u_1}{\partial t} = D_u \frac{\partial^2 u_1}{\partial x^2} + f_u u_1 + f_v v_1, \tag{7}$$

$$\frac{\partial v_1}{\partial t} = D_v \frac{\partial^2 v_1}{\partial x^2} - f_u u_1 - f_v v_1, \tag{8}$$

where

$$f_u = \frac{\partial f}{\partial u} = \frac{a_1(A_2 - 1)}{(1 + A_2)^3}, \quad f_v = \frac{\partial f}{\partial v} = \frac{a_1 A_2 (A_2^2 + 3A_2 + 4)}{(1 + A_2)^3},$$

denote partial derivatives of the reaction term computed at the basic solution. As we are interested in the description of the structure of the finite spatial size (i.e., finite wavelength k) consider a spatially periodic perturbation of the form

$$u_1 = U \exp(\sigma t + ikx), \quad v_1 = V \exp(\sigma t + ikx),$$

where U, V denote the perturbation amplitude and σ is the growth rate.

3.2 Dispersion relation

Substitution of the above expressions into (7,8) transforms the partial differential equations into a system of linear algebraic equations

$$\sigma U = -k^2 D_u U + f_u U + f_v V, \tag{9}$$
$$\sigma V = -k^2 D_v V - f_u U - f_v V. \tag{10}$$

Introducing the perturbation amplitude vector $\{U, V\}$ we rewrite them as a vector equation

$$\sigma \begin{pmatrix} U \\ V \end{pmatrix} = \begin{pmatrix} f_u - D_u k^2 & f_v \\ -f_u & -f_v - D_v k^2 \end{pmatrix} \begin{pmatrix} U \\ V \end{pmatrix} = \mathbf{J} \begin{pmatrix} U \\ V \end{pmatrix}, \tag{11}$$

where $\mathbf{J}$ denotes the Jacobian matrix. The explicit form of this matrix reads:

$$\mathbf{J} = \frac{1}{(1 + A_2)^3} \begin{pmatrix} a_1(A_2 - 1) - (1 + A_2)^3 D_u k^2 & a_1 A_2 (A_2^2 + 3A_2 + 4) \\ -a_1(A_2 - 1) & -a_1 A_2 (A_2^2 + 3A_2 + 4) - (1 + A_2)^3 D_v k^2 \end{pmatrix}. \tag{12}$$

The values σ satisfying this equation are called *eigenvalues* of the square Jacobian matrix $\mathbf{J}$, while the corresponding vectors $\{U, V\}$ are called *eigenvectors* of the same matrix.

Equation (11) can be also written as

$$(\mathbf{J} - \sigma\mathbf{I}) \begin{pmatrix} U \\ V \end{pmatrix} = \begin{pmatrix} 0 \\ 0 \end{pmatrix}, \tag{13}$$

where $\mathbf{I}$ denotes the two-dimensional identity matrix. This equation has a nonzero solution only if the determinant of the matrix in the l.h.s. of (13) equals zero:

$$\det(\mathbf{J} - \sigma\mathbf{I}) = 0. \tag{14}$$

The last condition rewrites into

$$\begin{vmatrix} a_1(A_2 - 1) - (1 + A_2)^3(D_u k^2 + \sigma) & a_1 A_2(A_2^2 + 3A_2 + 4) \\ -a_1(A_2 - 1) & -a_1 A_2(A_2^2 + 3A_2 + 4) - (1 + A_2)^3(D_v k^2 + \sigma) \end{vmatrix} = 0,$$

that relates the growth rate σ to the wavenumber k; it is called the *dispersion relation*. The explicit form of the dispersion relation is given by the quadratic equation for the growth rate:

$$\sigma^2 + \sigma(f_v - f_u + k^2 D_u + k^2 D_v) + k^2(D_u f_v - D_v f_u + k^2 D_u D_v) = 0. \tag{15}$$

This equation has two roots

$$\sigma_\pm = \frac{-a_1 - k^2(D_u + D_v) \pm \sqrt{D}}{2}, \tag{16}$$

$$D = [a_1 + k^2(D_v - D_u)]^2 + 4a_1 k^2(D_v - D_u)\frac{A_2 - 1}{(1 + A_2)^3}. \tag{17}$$

Direct computation shows that the determinant D in (17) is always positive so that both eigenvalues representing the growth rate are real. It means that the perturbation has a stationary spatially periodic profile and the oscillatory perturbations are not allowed. Inspection of (16) shows that σ_- is always negative.

Substituting the eigenvalues $\sigma_\pm$ into (11) we find the corresponding eigenvectors $\{U_\pm, V_\pm\}$. Thus the perturbations u_1, v_1 can be written as the linear superposition

$$u_1 = A_+ U_+ \exp(\sigma_+ t + ikx) + A_- U_- \exp(\sigma_- t + ikx) + c.c., \tag{18}$$

$$v_1 = A_+ V_+ \exp(\sigma_+ t + ikx) + A_- V_- \exp(\sigma_- t + ikx) + c.c., \tag{19}$$

where $A_\pm$ are the complex amplitudes, k is the perturbation profile wavenumber and *c.c.* denotes complex conjugation. It should be underlined that in the linear stability analysis the amplitude values are defined to the arbitrary nonzero factor.

The eigenvalue σ_- is always negative, so that the corresponding perturbation component decreases with time and can be completely neglected at large times $t \gg 1/|\sigma_-|$. When the other eigenvalue σ_+ is positive the corresponding component grows, the dynamics of its amplitude A_+ is the subject of weakly nonlinear analysis presented below.

3.3 Fastest growing mode

As it seen from Figure 1(a) the dependence of the growth rate σ_+ on the wavenumber k is non-monotonous and has a maximum $\sigma_+ = \sigma_m$ which corresponds to the *fastest* growing mode.

It is instructive to find the value k_m of the wavenumber at which this maximum σ_m is reached. At this point the derivative vanishes $\sigma'(k_m) = 0$. Differentiating the dispersion relation (15) with respect to square of wavenumber k and equating it to zero we find

$$\sigma(D_u + D_v) + D_u f_v - D_v f_u + 2k^2 D_u D_v = 0,$$
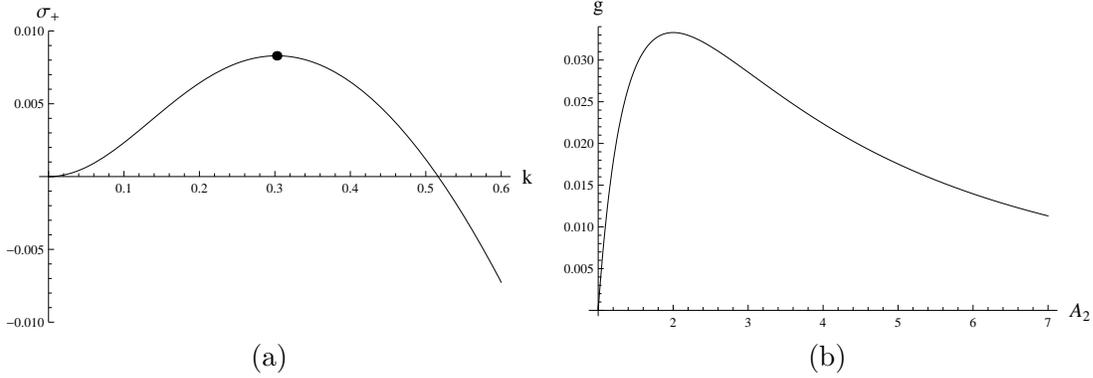
Figure 1: (a) The dispersion relation curve determines the dependence of the growth rate $\sigma_+(k)$ on the wavenumber for $a_1 = 1$, $A_2 = 2$, $D_u = 0.1$, $D_v = 10$. The dot shows the maximal growth rate σ_m of the fastest growing mode. (b) The function $g(A_2)$ in (22) reaches maximum $g_{max} = 0.033$ at $A_2 = 2$. The diffusion ratio D_u/D_v cannot exceed this value in order to have symmetry breaking possible.

from which we arrive at the relation

$$\sigma_m = \frac{D_v f_u - D_u f_v - 2k_m^2 D_u D_v}{D_u + D_v}. \tag{20}$$

Equating the expression for σ_+ given by (16) to the maximal value σ_m in (20) we find the relation for k_m

$$
\begin{aligned}
k_m^2 &= \frac{(D_v + D_u)\sqrt{f_v f_u} - (f_u + f_v)\sqrt{D_v D_u}}{(D_v - D_u)\sqrt{D_v D_u}} \\
&= \frac{a_1}{(A_2 + 1)^3} \cdot \frac{(D_v + D_u)\sqrt{A_2(A_2^2 + 3A_2 + 4)(A_2 - 1)} - [(A_2 + 1)^3 + 2(A_2 - 1)]\sqrt{D_v D_u}}{(D_v - D_u)\sqrt{D_v D_u}}.
\end{aligned} \tag{21}
$$

As the denominator in (21) is positive due to difference of the diffusivities of the protein forms $D_u \ll D_v$, we have to require positiveness of the numerator to obtain nonzero real value for the fastest growing mode wavenumber. This condition can be written as

$$\frac{D_v D_u}{(D_v + D_u)^2} \approx \frac{D_u}{D_v} < \frac{f_v f_u}{(f_v + f_u)^2} = \frac{A_2(A_2^2 + 3A_2 + 4)(A_2 - 1)}{[(A_2 + 1)^3 + 2(A_2 - 1)]^2} = g(A_2), \tag{22}$$

where we neglect D_u compared to D_v in the left fraction denominator. The function $g(A_2)$ shown in Figure 1(b) reaches its maximum $g_{max} = 28/841 \approx 0.033$ at $A_2 = 2$, so that this value determines the maximal value of the diffusivities ratio D_u/D_v for which one can observe symmetry breaking.

Substitution of the expression (21) into the formula (20) gives a simple symmetric formula for the maximal growth rate

$$\sigma_m = \frac{\left(\sqrt{D_v f_u} - \sqrt{D_u f_v}\right)^2}{D_v - D_u}. \tag{23}$$

The numerator in (20) should be positive that implies a condition

$$D_v f_u > D_u f_v. \tag{24}$$

7

Introduce two positive parameters ϵ and ϕ given by the ratios

$$\epsilon^2 = \frac{D_u}{D_v}, \ 0 < \epsilon \ll 1, \ \ \phi^2 = \frac{f_v}{f_u} = \frac{A_2(A_2^2 + 3A_2 + 4)}{A_2 - 1} > 0. \tag{25}$$

The value of ϕ depends on the only bifurcation parameter A_2 and it is real for $A_2 > 1$, while ϵ is determined by the diffusivities of the protein forms, so that these parameters describe two independent (reactive and diffusive) parts of the model system. The maximal growth rate σ_m in (20) can be rewritten as

$$\sigma_m = \frac{D_v f_u (1 - \sqrt{D_u f_v / D_v f_u})^2}{D_v - D_u} = f_u \frac{(1 - \epsilon\phi)^2}{1 - \epsilon^2} \approx f_u(1 - \epsilon\phi)^2 = \frac{a_1(A_2 - 1)}{(1 + A_2)^3}(1 - \epsilon\phi)^2. \tag{26}$$

This result implies that one has linear instability of the basic solution at $A_2 > 1$. The relation (21) for the wavenumber k_m reads in the same approximation

$$k_m^2 = \frac{f_u}{D_v} \cdot \frac{(1 - \epsilon\phi)(\phi - \epsilon)}{\epsilon} = \frac{f_u}{D_u} \cdot \epsilon\phi(1 - \epsilon\phi) = \frac{a_1(A_2 - 1)}{D_u(1 + A_2)^3} \cdot \epsilon\phi(1 - \epsilon\phi). \tag{27}$$

The condition (24) reduces to $\epsilon\phi < 1$, while from (22) we find

$$\epsilon < \frac{\phi}{1 + \phi^2} \Rightarrow \epsilon\phi < \frac{\phi^2}{1 + \phi^2} < 1,$$

so that the condition (24) satisfied identically.

Thus the symmetry breaking condition (22) for the Turing type bifurcation in the mass-conserved reaction-diffusion system has form

$$\epsilon < \frac{\phi}{1 + \phi^2}. \tag{28}$$

It establishes the relation between the diffusion (ϵ) and reaction (ϕ) part of the model required for the symmetry breaking. From the equation (11) at $k = k_m$ and $\sigma = \sigma_\pm$ find the eigenvectors

$$\{U_+, V_+\} = \{\phi/\epsilon, -1\}, \qquad \{U_-, V_-\} = \{\epsilon\phi, -1\}. \tag{29}$$

It can be checked by direct computation that the minimal value of ϕ is reached for $A_2 = 2$ and it equals to $\phi_{min} = 2\sqrt{7} \approx 5.29$, so that the ratio of perturbation amplitudes for the active u and inactive v forms is ϕ/ϵ which is larger than $\phi^2 = 28$.

4 Weakly nonlinear analysis

4.1 Galerkin expansion

To determine the approximate dynamics of the perturbation we use the Galerkin method [12] and start with the extended expansions of the protein concentrations into superposition of basic uniform profile, spatially periodic wave of the leading spatial wavenumber k_m corresponding to the fastest growing mode and an additional component:

$$u = u_0 + A_+(t)U_+ \exp(ik_m x) + A_-(t)U_- \exp(ik_m x) + u_2(t)\exp(2ik_m x) + c.c., \tag{30}$$

$$v = v_0 + A_+(t)V_+ \exp(ik_m x) + A_-(t)V_- \exp(ik_m x) + v_2(t)\exp(2ik_m x) + c.c., \tag{31}$$

where $u_2(t)$ and $v_2(t)$ denote the contribution to the perturbation corresponding to double harmonics. The expressions (30,31) are substituted into the original equations (1,2) expanded into series

up to the second order in perturbation amplitude. This expansion contains second order partial derivatives of the reaction term computed at the basic solution. Direct computation shows that all these derivatives are equal to each other and given by

$$F = f_{uu} = f_{vv} = f_{uv} = f_{vu} = -\frac{2a_1 A_2(A_2 - 2)}{C(1 + A_2)^4}.$$

Collecting the coefficients of the leading harmonics $\exp(ik_m x)$ we obtain a set of ordinary differential equations (ODEs) for the functions $A_+(t), A_-(t)$ presented below

$$A'_+ U_+ + A'_- U_- = \sigma_m A_+ + \sigma_- A_- + FM, \tag{32}$$
$$A'_+ V_+ + A'_- V_- = \sigma_m A_+ + \sigma_- A_- - FM, \tag{33}$$

where prime denotes time derivative and the parameter M is given by

$$M = (u_2 + v_2)[(U_+ + V_+)A_+^* + (U_- + V_-)A_-^*]. \tag{34}$$

Retaining the double harmonic terms proportional to $\exp(2ik_m x)$ we have the ODEs for $u_2(t), v_2(t)$ dynamics

$$u'_2 = (f_u - 4k_m^2 D_u)u_2 + f_v v_2 + FN, \tag{35}$$
$$v'_2 = -f_u u_2 + (-f_v - 4k_m^2 D_v)v_2 - FN, \tag{36}$$
$$N = [(U_+ + V_+)A_+ + (U_- + V_-)A_-]^2/2. \tag{37}$$

The system of four equations (32,33,35,36) with initial conditions $A_+(0) = A_{+0} \ll 1, A_-(0) = A_{-0} \ll 1, u_2(0) = v_2(0) = 0$, can be solved numerically to find the dynamics of the perturbation amplitudes. This is great simplification as the numerical solution of ODEs is much faster and more stable than the direct simulation of the original problem.

Nevertheless one can go even further along the road of perturbation dynamics analysis and obtain a closed equation describing the evolution of the basic perturbation amplitude A_+ only.

4.2 Derivation of Landau equation

Assuming that the dynamics of the second harmonics components reaches its steady state much faster than the leading perturbation does, we set the derivatives of the amplitudes u_2, v_2 equal to zero and find these amplitudes

$$u_2 = D_v K A_+^2, \ v_2 = -D_u K A_+^2, \ K = \frac{F(U_+ + V_+)^2}{2(4k_m^2 D_u D_v + D_u f_v - D_v f_u)}, \tag{38}$$

where we neglected the vanishing terms proportional to A_-.

Using methods of linear algebra from the equations (32,33) one can find the equation for the amplitude A_+ of the fastest growing mode. In order to do it we first note that the l.h.s. of equations (32,33) can be written in the matrix form

$$\begin{pmatrix} A'_+ U_+ + A'_- U_- \\ A'_+ V_+ + A'_- V_- \end{pmatrix} = \begin{pmatrix} U_+ & U_- \\ V_+ & V_- \end{pmatrix} \begin{pmatrix} A'_+ \\ A'_- \end{pmatrix} = \mathbf{P} \begin{pmatrix} A'_+ \\ A'_- \end{pmatrix},$$

where the matrix $\mathbf{P}$ is made of the eigenvectors of the Jacobian matrix. The equations (32,33) read

$$\mathbf{P} \begin{pmatrix} A'_+ \\ A'_- \end{pmatrix} = \sigma_m A_+ \begin{pmatrix} U_+ \\ V_+ \end{pmatrix} + \sigma_- A_- \begin{pmatrix} U_- \\ V_- \end{pmatrix} + F \begin{pmatrix} M \\ -M \end{pmatrix}. \tag{39}$$

Multiplying (39) from the left by the inverse matrix $\mathbf{P}^{-1}$ we find the solution

$$\begin{pmatrix} A'_+ \\ A'_- \end{pmatrix} = \sigma_m A_+ \mathbf{P}^{-1} \begin{pmatrix} U_+ \\ V_+ \end{pmatrix} + \sigma_- A_- \mathbf{P}^{-1} \begin{pmatrix} U_- \\ V_- \end{pmatrix} + F\mathbf{P}^{-1} \begin{pmatrix} M \\ -M \end{pmatrix}, \tag{40}$$

Denote the elements of the matrix $\mathbf{P}^{-1}$

$$\mathbf{P}^{-1} = \begin{pmatrix} \hat{p}_{11} & \hat{p}_{12} \\ \hat{p}_{21} & \hat{p}_{22} \end{pmatrix}.$$

From the definition of the inverse matrix it is easy to check by direct computation that $\hat{p}_{11}U_+ + \hat{p}_{12}V_+ = 1$ and $\hat{p}_{11}U_- + \hat{p}_{12}V_- = 0$. It leads to the explicit expressions

$$\hat{p}_{11} = -\frac{V_-}{V_+U_- - U_+V_-}, \quad \hat{p}_{12} = \frac{U_-}{V_+U_- - U_+V_-}. \tag{41}$$

Then from (40) we find

$$A'_+ = \sigma_m A_+ + (\hat{p}_{11} - \hat{p}_{12})FM = \sigma_m A_+ - \frac{U_- + V_-}{V_+U_- - U_+V_-}FM. \tag{42}$$

Neglecting the amplitude A_- we set it equal to zero to find

$$M = (u_2 + v_2)(U_+ + V_+)A_+^*.$$

Using here the expressions (38) we obtain

$$M = (D_v - D_u)(U_+ + V_+)K|A_+|^2 A_+, \tag{43}$$

where

$$K = \frac{F(U_+ + V_+)^2(D_v - D_u)}{2[4(D_v + D_u)\sqrt{D_uD_vf_uf_v} - D_u^2f_v - D_v^2f_u - 3D_uD_v(f_u + f_v)]}.$$

Substituting the relation (43) into (42) we obtain the amplitude *Landau equation*

$$A'_+ = \sigma_m A_+ + \kappa|A_+|^2 A_+, \tag{44}$$

where the coefficient of the nonlinear term κ is called the *Landau coefficient*. The explicit expression of the coefficient reads

$$\kappa = -\frac{(U_- + V_-)(U_+ + V_+)^3}{V_+U_- - U_+V_-} \cdot \frac{F^2(D_v - D_u)^2}{2[4(D_v + D_u)\sqrt{D_uD_vf_uf_v} - D_u^2f_v - D_v^2f_u - 3D_uD_v(f_u + f_v)]}. \tag{45}$$

The expressions (45) and (29) imply that the Landau coefficient is homogeneous function of the diffusion coefficients D_u, D_v. It is instructive to represent it through the ratios ϵ and ϕ. The first factor in the expression (45) reads

$$\frac{(U_- + V_-)(U_+ + V_+)^3}{V_+U_- - U_+V_-} = -\frac{(\phi - \epsilon)^3(1 - \epsilon\phi)}{(1 - \epsilon^2)\epsilon^2\phi} \approx -\frac{(\phi - \epsilon)^3(1 - \epsilon\phi)}{\epsilon^2\phi},$$

while the second one converts into

$$\frac{F^2(1 - \epsilon^2)^2}{2f_u[4(1 + \epsilon^2)\epsilon\phi - \epsilon^4\phi^2 - 1 - 3\epsilon^2(1 + \phi^2)]} \approx -\frac{F^2}{2f_u(1 - \epsilon\phi)(1 - 3\epsilon\phi)}.$$

The final expression for the Landau coefficient reads

$$\kappa = -F^2 \frac{(\phi - \epsilon)^3}{2 f_u \epsilon^2 \phi(1 - 3\epsilon\phi)}. \tag{46}$$

Recalling the expression (26) for the maximal growth rate we find the value of the Landau coefficient

$$\kappa = -\frac{2 a_1 a_2^2 (A_2 - 2)^2}{(A_2 - 1)(1 + A_2)^5} \cdot \frac{(\phi - \epsilon)^3}{\epsilon^2 \phi(1 - 3\epsilon\phi)} = -\frac{F^2}{2\sigma_m} \cdot \frac{(\phi - \epsilon)^3 (1 - \epsilon\phi)^2}{\epsilon^2 \phi(1 - 3\epsilon\phi)}. \tag{47}$$

When $A_2 = 2$ the Landau coefficient vanishes and one has to use expansion to higher harmonics to find the equation governing the perturbation dynamics; we do not consider this degenerate case as it goes beyond the scope of this communication.

4.3 Amplitude equation analysis

As the Landau coefficient is a real number one can replace the complex perturbation amplitude by its real part and the Landau equation reads

$$A'_+ = \sigma_m A_+ + \kappa A_+^3, \tag{48}$$

where both the linear growth rate σ_m and amplitude A_+ are positive. The sign of the Landau coefficient κ determines the perturbation amplitude dynamics. For the positive κ the amplitude undergoes infinite growth that eventually breaks the assumption about the smallness of the perturbation. In this case actual emerging steady state (if it exists) can be found by the direct numerical simulations of the original problem (1,2).

In addition to this qualitative statement one can sometimes make important quantitative predictions. For example, in hydrodynamics of thin liquid films the uniform basic state corresponds to the film of constant thickness. Such a film can lose stability to small periodic perturbations with amplitude governed by the Landau equation with positive nonlinear term. It means that the perturbation will grow and its amplitude eventually will reach the initial film thickness at which moment the film ruptures. Using the Landau equation it is possible to estimate rupture time and its dependence of the systems parameters [12].

The negative Landau coefficient implies that the linear growth of the perturbation is balanced by the nonlinear term and eventually the amplitude saturates at the value

$$A_s = \sqrt{-\sigma_m/\kappa}. \tag{49}$$

Using formula (47) one obtains its explicit expression

$$A_s = \frac{\sigma_m}{|F|} \sqrt{\frac{2\epsilon^2 \phi(1 - 3\epsilon\phi)}{(\phi - \epsilon)^3 (1 - \epsilon\phi)^2}} = \frac{(A_2^2 - 1)C}{A_2|A_2 - 2|} \frac{\epsilon(1 - \epsilon\phi)}{\phi - \epsilon} \sqrt{\frac{2\phi(1 - 3\epsilon\phi)}{\phi - \epsilon}}. \tag{50}$$

which appears to scale with the linear growth rate σ_m. In this case the steady state is established representing a periodic structure with the wavelength equal to $L_m = 2\pi/k_m$. As the value A_s corresponds to the steady state perturbation amplitude of the inactive form, the corresponding value for the active form can be computed using (29) to give $A_s\phi/\epsilon$. Thus the steady state solution predicted by the weakly nonlinear analysis reads

$$u = u_0 + \frac{A_s\phi}{\epsilon} \cos k_m x, \tag{51}$$

$$v = v_0 - A_s \cos k_m x. \tag{52}$$

If the size of the cell L is much larger than L_m one can expect to observe a multiple peak periodic structure as the result of symmetry breaking. The decrease of the cell size to the value lower than $2L_m$ leads to survival of the unimodular profile.

It should be underscored that the existence of the stable periodic structure resulting in symmetry breaking of Turing type is possible when a certain condition on the parameters is met. This condition follows from the positiveness of the fraction under square root in (50). Assuming $\phi > \epsilon$ we write the existence condition for the stable periodic profile as

$$\epsilon\phi < 1/3. \tag{53}$$

The last relation determines the perturbation saturation condition and it can be expressed in the original parameters as

$$\frac{D_u A_2(A_2^2 + 3A_2 + 4)}{D_v(A_2 - 1)} < \frac{1}{9}. \tag{54}$$

Observation of the stable periodic profile also strongly depends on the initial and boundary conditions as well as on the value of the bifurcation parameter A_2. Analysis of (51) shows that in order to observe a multipeak periodic solution one has to satisfy a condition $u_0 > A_s\phi/\epsilon$, so that the value of the active form distribution never reaches zero.

Using (5) and (50) we obtain the condition of existence of the periodic steady state solution

$$\frac{A_2(A_2 + 2)C}{(A_2 + 1)^2} \geq \frac{(A_2^2 - 1)C}{A_2|A_2 - 2|} \frac{\phi(1 - \epsilon\phi)}{\phi - \epsilon} \sqrt{\frac{2\phi(1 - 3\epsilon\phi)}{\phi - \epsilon}},$$

which leads to

$$\frac{A_2^2|A_2^2 - 4|}{(A_2 - 1)(A_2 + 1)^3} \geq \frac{\phi(1 - \epsilon\phi)}{\phi - \epsilon} \sqrt{\frac{2\phi(1 - 3\epsilon\phi)}{\phi - \epsilon}}. \tag{55}$$

Neglecting ϵ compared to ϕ we rewrite the condition (55) as

$$\frac{A_2^2|A_2^2 - 4|}{(A_2 - 1)(A_2 + 1)^3} \geq (1 - \epsilon\phi)\sqrt{2(1 - 3\epsilon\phi)}. \tag{56}$$

The ratio ϕ itself depends on A_2 as shown in (25) so that the last condition for given value of ϵ determines the range of ϕ values for which the periodic steady state solution exists as depicted in Figure 2.

For $u_0 < A_s\phi/\epsilon$ the multipeak periodic solution breaks as in such a case the value u of active form can reach zero and the assumption (30) about periodic solution fails. When the problem (1-4) is simulated numerically, strong nonlinearities of a transient solution arising in computation lead to removal of majority of the peaks and the steady state solution has one or two peaks (depending on the size of the cell). The single peak steady state solution was reported in both [5] and [4] where the authors restrict consideration to the linear stability analysis and numerical simulations only.

5   Numerical simulations

To confirm conclusions of weakly nonlinear analysis in this section we present results of numerical simulations of the model (1-4) for different sets of problem parameters corresponding to four types of qualitatively distict solutions. The whole range of the bifurcation parameter A_2 value can be split into four respective regions. Below we discuss these regions and their characteristic solutions.
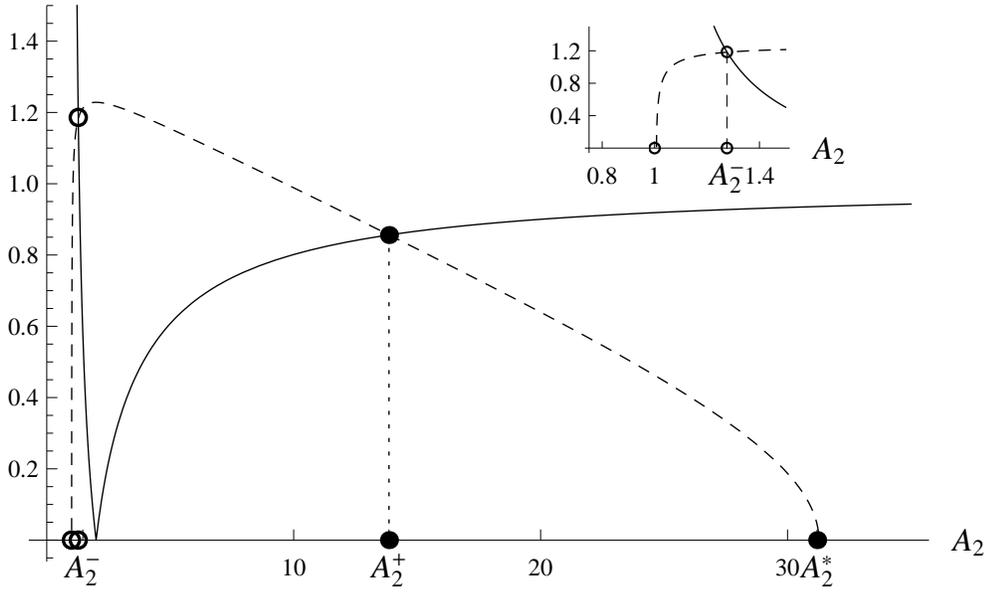
Figure 2: Computation of the bifurcation parameter A_2 range where the periodic steady state solution exists for $\epsilon = 0.01$. A solid line represents the l.h.s. of the inequality (56); the r.h.s. of this condition is shown by a dashed curve. The inset shows enlarged and rescaled left portion of the main figure. There are two ranges of allowed values of the bifurcation parameter – a very narrow one between the empty circles with $A_2 \approx 1$ (see inset) and a larger one between the filled circles with $A_2 \gg 1$. The definition of the critical values $A_2^- = 1.26$ $A_2^+ = 13.86$ and $A_2^* = 31.2$ are given in the text.

1. $0 < A_2 < 1$. In this region the basic solution is linearly stable to small perturbations. This behavior is shown in Figure 3(a).

2. $A_2 > A_2^*$, where A_2^* satisfies the relation $3\epsilon\phi(A_2^*) = 1$. This range corresponds to linear instability but the saturation condition (54) does not hold. It leads to growth of small perturbation beyond the limitations of weakly nonlinear analysis, so the steady state can be determined by numerical simulations only. An example is given in Figure 3(b).

3. $A_2^- < A_2 < A_2^+$, where $A_2^\pm$ satisfy the equality in relation (56). In this case the saturation condition (54) holds, but the saturated amplitude of the perturbation of active form is larger than the basic value u_0. As the result a small initial amplitude of periodic multipeak profile grows until the amplitude reaches zero at some location. At this moment small nonlinearity is replaced by a larger one, the profile is no longer harmonic. As the resluts of strong nonlinearities arising in numerical simulation due to numerical errors nearly all peaks of the initial multipeak profile may disappear and only a single peak survives. This behavior was reported in numerical simulations in [5, 4]. When the cell size L is much larger compared to the periodic structure wavelength may also can observe more than one peak in the steady state solution. The corresponding dynamics is presented in Figure 3(c).

4. $1 < A_2 < A_2^-$ and $A_2^+ < A_2 < A_2^*$. This case is characterized by the establishment of the steady state periodic multipeak profile with the amplitude predicted by weakly nonlinear analysis formula (50). The amplitude of the active form profile is smaller than the basic value u_0. The growth of small initial amplitude saturates and the multipeak profile survives. The

corresponding dynamics is shown in Figure 3(d).
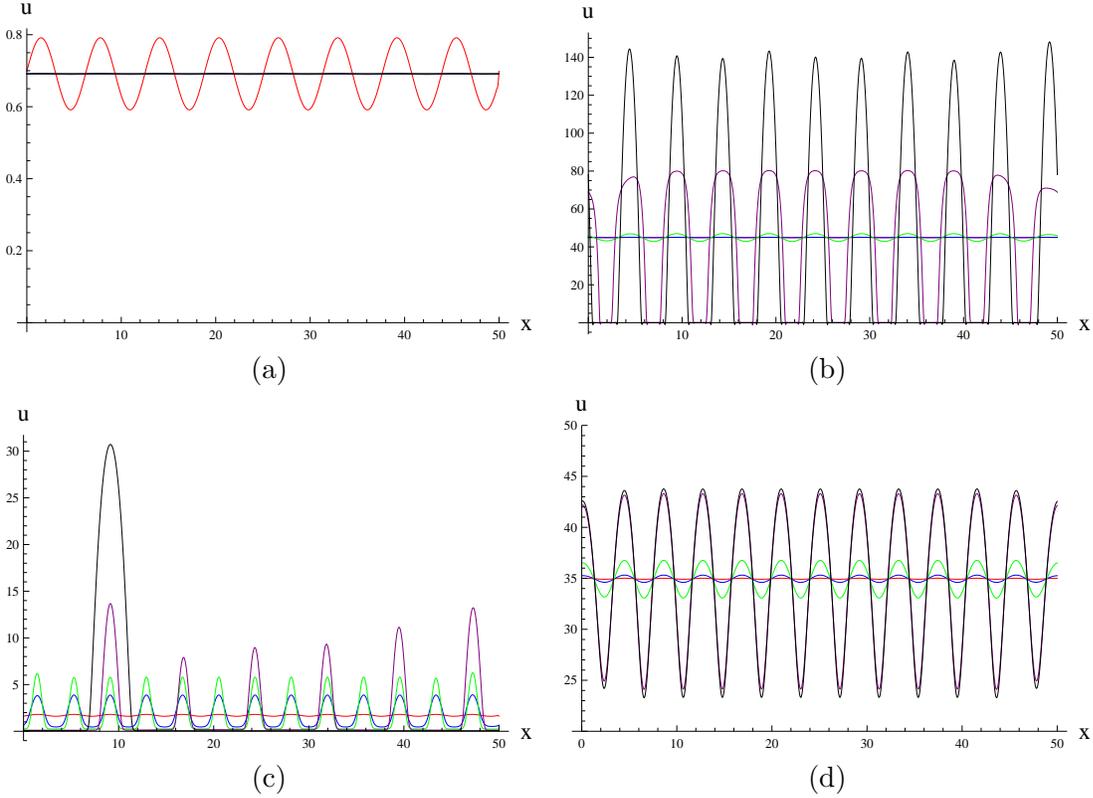
Figure 3: Evolution of numerical solution for the active form amplitude u of the system (1-4) with periodic boundary conditions and initial conditions (5) with the following parameter values are $a_1 = 1$, $a_2 = 0.8$, $L = 50$, $\epsilon = 0.01$, $D_v = 1$, $D_u = \epsilon^2$. (a) The basic state is linearly stable and small periodic perturbations decrease fast ($C = 1$, $A_2 = 0.8$). (b) The perturbation amplitude does not staturate that leads to emergence of nonlinear periodic profile ($C = 45$, $A_2 = 36$). (c) Small periodic perturbation grows until it reaches zero at some location leading to strong nonlinearity followed by disappearance of some peaks ($C = 2$, $A_2 = 1.6$). (d) Small periodic perturbation grows until it saturates at steady state multipeak periodic profile with the amplitude predicted by weakly nonlinear theory ($C = 35$, $A_2 = 28$).

6   Discussion

The choice of the model describing cell polarization following symmetry breaking is dictated by several principles among which are simplicity of the model and its ability to predict the observed behavior of live cells. The first principle requires a selection of the major players in a system of interacting proteins that determine the polarization process. Usually the original model is based on several interacting elements of complex biochemical nature that are determined by known physical interactions at a given physiological stage of the cell. Most of these components are assumed to be driven by a few proteins governing the system dynamics. The extreme version of this approach involves selection of a single protein existing in two forms – active and inactive. For instance, the active form can be associated with the cell membrane while the inactive one belongs to the

14

cytosolic pool, so the diffusivity of these two forms may differ by several orders of magnitude. The important natural feature of these models is the mass conservation of the governing protein. It was shown in previous publications that the mass-conserved reaction-diffusion models demonstrate a rich spectrum of dynamics including the Turing type bifurcation and the wave-pinning mechanism of symmetry breaking. It should be noted that these minimalistic models, despite being an extreme simplification of the cell dynamics, still grasp some important features of polarization process. However, it is important to find out boundaries of applicability of such models for description of real biological cellular systems, as well as to develop new realistic models of this type.

Dynamics stability analysis of theoretical models describing symmetry breaking leading to cell polarization is important for verification of the model applicability. It consists of several consecutive steps starting with determination of the basic uniform steady state and linear analysis of stability of this basic state. The result of this step is a set of conditions imposed on the model parameters required for symmetry breaking. The dynamics of the perturbation to the basic state can be considered analytically using the weakly nonlinear analysis approach. This step enables prediction of the parameter values for which the amplitude of the perturbation saturates to some finite value leading to establishment of the new stationary periodic structure. It can be done by analysis of the nonlinear term in the Landau equation for the perturbation amplitude.

Application of the linear and weakly nonlinear analyses to the mass-conserved reaction-diffusion model is possible due to the mathematical simplicity of this model. In this communication using the model proposed in [5] as an example we derive the conditions required for the Turing type symmetry breaking and determine the linear growth rate for a finite wavelength periodic perturbation. We also determine the range of parameter values defining the diffusive properties of both protein forms as well as the reaction part of the model for which the saturation of the perturbation amplitude can be reached. We find the explicit expression for the saturation amplitude and show that it is linearly proportional to the linear growth rate determined at the linear stability analysis step.

The weakly nonlinear analysis presented in this communication assumes that the perturbation amplitude is spatially uniform and its spatial modulation can be neglected. This assumption can be dropped and the resulting equation will have form of more general *Ginzburg-Landau equation* having additional amplitude diffusion term. This equation is widely used in systems analysis [13] including pattern formation so important in nonlinear science. The Ginzburg-Landau equation admits the spatially uniform solution presented in this communication, but now the stability of this solution can be broken due to presence of the diffusive term. In order to figure out the conditions of this *secondary instability* one has to perform the linear stability analysis on the Ginzburg-Landau equation itself.

The weakly nonlinear analysis for reaction-diffusion model with larger number of variables or in higher spatial dimension is much more complicated compared to one presented here, as it requires very cumbersome computations. One possible approach to resolve this complexity issue is the usage of modern computer algebra software to perform this analysis in general form [14] and then to apply the general formulas to a specific model.

Acknowledgments

References

[1] Iden S and Collard J G 2008 Crosstalk between small GTPases and polarity proteins in cell polarization *Nat Rev Mol Cell Biol* **9** 846-859

[2] Slaughter B S, Smith S E and Li R 2009 Symmetry breaking in the life cycle of the budding yeast *Cold Spring Harb Perspect Biol* 1-17

[3] Onsum M D and Rao C V 2009 Calling heads from tails: the role of mathematical modeling in understanding cell polarization *Current Opinion in Cell Biology* **21** 74-81

[4] Jilkine A and Edelstein-Keshet L 2011 A comparison of mathematical models for polarization of single eukariotic cells in response to guided cues *PLoS Computational Biology* **7** e1001121

[5] Otsuji M, Ishihara S, Co S, Kaibuchi K, Mochizuki A and Kuroda S 2007 A mass conserved reaction-diffusion system captures properties of cell polarity *PLoS Computational Biology* **3** e108

[6] Goryachev A B and Pokhilko A V 2008 Dynamics of Cdc42 networkembodies Turing-type mechanism of yeast cell polarity *FEBS Letters* **582** 1437-1443

[7] Mori Y, Jilkine A and Edelstein-Keshet L 2010 Asymptotic and bifurcation analysis of wave-pinning in reaction-diffusion model for cell polarization *SIAM J. Appl. Math.* **71** 1401-1427

[8] Crawford J D 1991 Introduction to bifurcation theory *Rhys. Mod. Rev.* **63** 991-1037

[9] Murray J D 2003 Mathematical Biology I: An Introduction. Springer, 3rd ed.

[10] Cross M C and Hohenberg P C 1993 Pattern formation outside of equilibrium *Rhys. Mod. Rev.* **65** 851-1112

[11] Ridley A J, Schwartz M A, Burridge K, Firtel R A, Ginsberg M H, Borisy G, Parsons J T and Horwitz A R 2003 Cell migration: integrating signals from front to back *Science* **302** 1704-1709

[12] Rubinstein B Y and Lishansky A M 2011 Rupture of thin liquid films: generalization of weakly nonlinear theory *Phys Rev E* **83** 031603

[13] Aranson I S and Kramer L 2002 The world of the complex Ginzburg-Landau equation *Rev. Mod. Phys.* **74** 99-143

[14] Pismen L M and Rubintein B Y 1999 Computer tools for bifuraction analysis: general approach with application to dynamical and distributed systems *Int. J. Bifurcation and Chaos* **9** 983-1008